Performance trade-offs in holographic recording in LiNbO$_3$ crystals

Ali Adibi

Georgia Institute of Technology, School of Electrical and Computer Engineering, Atlanta, GA 30332, USA

adibi@ee.gatech.edu

Karsten Buse

Universität Bonn, Physikalisches Institut, Wegelerstr. 8, D-53115 Bonn, Germany

kbuse@uni-bonn.de

Demetri Psaltis

California Institute of Technology, Department of Electrical Engineering, Pasadena, California 91125, USA

psaltis@sunoptics.caltech.edu

Abstract: We use the quantitative measures for dynamic range, sensitivity, and persistence in holographic recording to compare the performance of singly–doped and doubly–doped LiNbO$_3$ crystals. We explain the trade-offs among the performance measures in both singly–doped and doubly–doped crystals. We show that the range of performance that can be obtained using doubly–doped crystals is much larger than that obtained using singly–doped ones.

© 2001 Optical Society of America

OCIS codes: (090.2900) Holographic recording materials, (090.7330) Volume holographic gratings; (160.3730) Lithium niobate; (210.0210) Optical data storage

1 Introduction

Several holographic storage demonstrations using iron–doped lithium niobate (LiNbO$_3$:Fe) were presented in the last few years [1, 2, 3]. Erasure of the holograms during read–out has been one of the major problems in the practical realization of holographic read/write memories. We recently proposed and demonstrated the two–center holographic recording method to solve this problem by using doubly–doped LiNbO$_3$ [4, 5]. Several aspects of persistent holographic storage in doubly–doped LiNbO$_3$ (i.e., hologram multiplexing [6], sensitivity improvement [7], optimization [5, 8], and the role of different dopants [9, 10, 11]) were investigated. In this paper, we present a framework for the comparison of the performances of singly–doped and doubly–doped LiNbO$_3$ crystals for holographic storage. We show that by going from singly–doped crystals to doubly–doped crystals, we add one degree of freedom in the optimization of the performance for holographic storage. We show that the range of performance characteristics that can be obtained using a doubly–doped crystal is much larger than that obtained using a singly–doped one. We also explain the major trade–offs among dynamic range, sensitivity, and persistence in holographic storage in LiNbO$_3$ crystals.

2 Performance Measures in Holographic Recording

The main performance measures in holographic recording are dynamic range ($M/\#$) [12], sensitivity (S) [13], and persistence ($R/\#$) [14]. The measures for the dynamic range ($M/\#$) and sensitivity (S) are defined as

$$M/\# \;=\; \frac{A_0 \tau_{\mathrm{e}}}{\tau_{\mathrm{r}}}\,, \tag{1}$$

$$S \;=\; \frac{\dfrac{d\sqrt{\eta}}{dt}\big|_{t=0}}{I_{\mathrm{Rec}} L} \;=\; \frac{A_0/\tau_{\mathrm{r}}}{I_{\mathrm{Rec}} L}\,. \tag{2}$$

In these equations, A_0 is the saturation hologram strength, η is diffraction efficiency, and τ_{r} and τ_{e} are recording and erasure time constants during multiplexing holograms, respectively. Note that by using $\sqrt{\eta} = A$ we assume that $\eta \ll 1$, which is the case when we multiplex several holograms. In hologram multiplexing experiments erasure of previously written holograms is caused by recording new holograms. The symbols I_{Rec} and L denote the total recording intensity and the thickness of the recording medium (or the hologram), respectively. If we multiplex M holograms in the same volume appropriately [15], each will have a diffraction efficiency equal to $\eta = [(M/\#)/M]^2$. Since $M/\#$ depends on the crystal thickness (L), we define a normalized dynamic range measure as

$$M'/\# \;=\; \frac{M/\#}{L}\,, \tag{3}$$

to normalize the effect of thickness similar to the normalization for S.

   We recently defined a measure for persistence ($R/\#$) by quantifying the erasure of a hologram during read–out in a reference system [14]. Such a system is composed of M holograms multiplexed in the same volume, and the minimum acceptable diffraction efficiency of each reconstructed plane–wave hologram is $\eta_{\min}$. We also assumed that in such a system, we need to have N_{ph} photons for each pixel with area $\mathcal{A}_{\mathrm{pixel}}$ at the detector to obtain an acceptable signal to noise ratio [16]. The measure for persistence, $R/\#$, is defined as the number of times we can read the information in the entire module (all M holograms) before the diffraction efficiency of each hologram falls below the minimum acceptable value ($\eta_{\min}$). The formula for $R/\#$ is given by [14]

$$R/\# \;\equiv\; \frac{(\tau_{\mathrm{e}}' I_{\mathrm{Rd}})\mathcal{A}_{\mathrm{pixel}}}{2M N_{\mathrm{ph}} h\nu}\left[\left(\frac{M/\#}{M}\right)^2 - \eta_{\min}\right] \tag{4}$$

$$\;=\; \frac{P\mathcal{A}_{\mathrm{pixel}}}{2M N_{\mathrm{ph}} h\nu}\left[\left(\frac{M/\#}{M}\right)^2 - \eta_{\min}\right],$$

where τ_{e}', I_{Rd}, and $P = \tau_{\mathrm{e}}' I_{\mathrm{Rd}}$ are erasure time constant during read-out, reading light intensity, and normalized erasure time constant, respectively. Note that τ_{e}' in Eq. 4 is, in general, different from τ_{e} in Eq. 1. The former is the erasure time constant of a hologram during read–out while the latter is the erasure time constant of a hologram during the recording of other holograms in the same location. In this paper, we assume that the dark erasure mechanisms such as dark conductivity and ionic compensation in dark are negligible compared to light–induced erasure. To measure $R/\#$ experimentally, we compute $P = \tau_{\mathrm{e}}' I_{\mathrm{Rd}}$ from erasure response of a hologram, and put the computed value along with the previously measured $M/\#$ into Eq. 4.

3   Performance Range in Singly–Doped and Doubly–Doped Crystals

In singly–doped crystals, $\tau_e I_{\text{Rec}}$ and $\tau_e' I_{\text{Rd}}$ are equal (or $\tau_e = \tau_e'$ for equal recording and reading intensities), since the physical erasure mechanisms during recording and reading in such crystals are the same. As a result, in singly–doped crystals, P (and therefore, $R/\#$) is totally dependent on $M/\#$ and S as shown below. By combining Eqs. 1, 2, and 3, we obtain

$$P \;=\; \frac{M/\#}{LS} = \frac{M'/\#}{S} \;. \tag{5}$$

This means that we can freely choose only two parameters from the trio of $M/\#$, S, and $R/\#$ in holographic recording in a singly–doped crystal. The simplified formulas for the variation of $M/\#$ and S of a singly–doped LiNbO$_3$:Fe crystal in the regime of the domination of bulk photovoltaic effect (for the case of congruently melting crystals) is

$$M/\# \;\propto\; \frac{\kappa_{\text{Fe}}\gamma_{\text{Fe}}}{q_{\text{Fe}}s_{\text{Fe}}}(N_{\text{Fe}} - N_{\text{Fe}}^-) \;, \tag{6}$$

$$S \;\propto\; \kappa_{\text{Fe}}N_{\text{Fe}}^- \;. \tag{7}$$

where $q_{\text{Fe}}s_{\text{Fe}}$, κ_{Fe}, and γ_{Fe} are absorption cross section for excitation of electrons form the Fe traps to the conduction band (at the recording wavelength), bulk photovoltaic constant of the Fe traps (at the recording wavelength), and recombination coefficient of the Fe traps, respectively. Furthermore, N_{Fe} and N_{Fe}^- are the total Fe concentration and the concentration of electrons in the Fe traps, respectively. Using Eqs. 5, 6, and 7 we obtain

$$P \;\propto\; \frac{\gamma_{\text{Fe}}}{q_{\text{Fe}}s_{\text{Fe}}}\frac{N_{\text{Fe}} - N_{\text{Fe}}^-}{N_{\text{Fe}}^-} \;. \tag{8}$$

In Eqs. 6 and 7, we only considered the important parameters that depend on the photorefractive (Fe) centers. In these equations, we neglected the light absorption through the crystal. For considerable absorption, both $M/\#$ and S are multiplied by $\exp(-\alpha L)$ with α being the intensity absorption coefficient of the crystal at the recording wavelength. From these equations, we can see that the trade–off between $M/\#$ and S can be performed by changing N_{Fe}^-, the electron concentration in the Fe traps. This can be performed by annealing (oxidation / reduction) of the crystal. However, the range of this trade–off is limited by the absorption of recording and reading light through the crystal. Increasing N_{Fe}^- beyond some limit results in large absorption coefficient α reducing both $M/\#$ and S.

One idea to extend the range of obtainable $M/\#$ and S is to use a doubly–doped crystal, for example LiNbO$_3$:Fe:Mn. Figure 1 compares the band diagram of a LiNbO$_3$:Fe crystal with that of a LiNbO$_3$:Fe:Mn crystal. Since Mn traps are deeper than Fe traps, electrons occupy Mn traps before Fe traps. By highly oxidizing a LiNbO$_3$:Fe:Mn crystal, we can have all the Fe traps as well as most of the Mn traps empty. The remaining electrons occupy a small portion of the Mn traps, and the crystal properties are similar to those of a highly oxidized LiNbO$_3$:Mn crystal. On the other hand, we can make all Mn traps as well as a large portion of the Fe traps filled with electrons by highly reducing the crystal. Such a crystal can act like a highly reduced LiNbO$_3$:Fe crystal. The properties of the LiNbO$_3$:Fe:Mn crystal at different oxidation / reduction state is between the two extreme mentioned above (from highly oxidized LiNbO$_3$:Mn to highly reduced LiNbO$_3$:Fe). Therefore, we
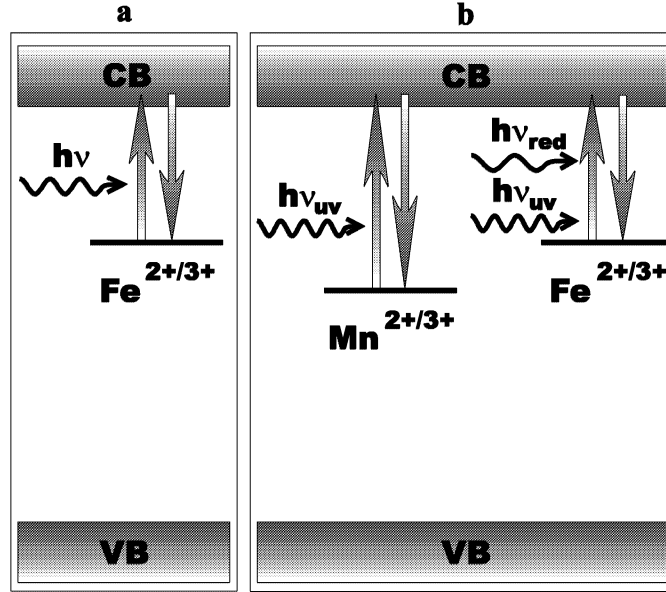
Fig. 1. Energy band diagram for a typical $LiNbO_3$ crystal doped with (a) Fe, and (b) Fe and Mn. CB, and VB stand for conduction band and valance band, respectively.

can generate an effective trap with tunable properties by using a doubly–doped crystal. In other words, depending on the doping concentration and oxidation / reduction state, the combination of the Fe traps and the Mn traps can be considered as an effective set of traps with properties between those of Fe and Mn traps.

If we use the light of only one wavelength for holographic recording in a $LiNbO_3$:Fe:Mn crystal, the previous relation between $M/\#$, S, and $R/\#$ (Eq. 5) still holds, since the erasure mechanisms during read–out and during recording other holograms are the same. However, the range of obtainable $M/\#$ and S is larger now due to the possibility of tuning the properties of the effective traps by annealing. To have more control over $M/\#$, S, and $R/\#$ and to be able to adjust all three measures independently instead of just two of them, we can use two–center holographic recording in a doubly–doped crystal [4]. To use a $LiNbO_3$:Fe:Mn crystal for two–center recording, we first need to oxidize the crystal properly [17] to have all Fe traps as well as a portion of the Mn traps initially empty. Two–center holographic recording is performed by a homogeneous UV beam for sensitization and two coherent beams (at longer wavelength) for recording. The basic idea of two–center holographic recording is to bring with the UV light electrons from Mn to Fe via the conduction band, to use these electrons to record the hologram with red or green light, and eventually to transfer the electrons from the Fe centers back to the Mn centers by red or green light. This results in a hologram stored in Mn centers that persists against further red or green illumination.

The unique property of two–center holographic recording is the distinction between the erasure time constant of a hologram during recording of other holograms (τ_e) and the erasure time constant during read–out of a hologram (τ_e'). The erasure of a hologram during the recording of other holograms is caused by the simultaneous presence of sensitizing (UV) and recording (red or green) beams. On the other hand, erasure of a hologram during read–out is caused only by the reading (red or green) beam, since the sensitizing (UV) beam is not present during read–out. Furthermore, the electron concentration in the shallower (Fe) traps is considerable during recording

(due to the sensitization process) while it is negligible (practically zero) during read–out (since the hologram is recorded in the Mn traps). Therefore, the erasure during read–out is much weaker than that during recording of other holograms (τ_e' is much larger than τ_e) in two–center recording in a doubly–doped crystal. Furthermore, τ_e' and τ_e are not proportional to each other, and Eq. 5 is not applicable to two–center recording. Therefore, we can trade–off all three of $M/\#$, S, and $R/\#$ in two–center recording instead of two ($M/\#$ and S) in normal recording. In other words, by using a doubly–doped crystal with two–center recording, we can obtain an additional degree of freedom (persistence) for our design.

4 Experiments

To verify the above–mentioned claims, we performed holographic recording and read–out experiments with two $LiNbO_3$:Fe:Mn crystals from the same boule each doped with 0.075 wt. % Fe_2O_3 and 0.01 wt. % MnO. Both crystals were first oxidized for 1 hour at $1000\,^\circ$C in O_2 atmosphere. The crystals were then reduced at $800\,^\circ$C in Ar atmosphere for either one hour (XTAL1) or four hours (XTAL2). All Fe traps in XTAL1 are empty while more than 90% of the Mn traps in this crystal are occupied by electrons. On the other hand, all Mn traps as well as a portion of Fe traps are initially occupied by electrons in XTAL2. With this annealing treatment XTAL1 is appropriate for persistent holographic recording (two–center recording) while XTAL2 is good for normal single wavelength recording with destructive read–out. Normal holographic recording (no sensitizing light present) was performed with two plane waves with equal intensities and ordinary polarization, while two–center recording (sensitizing light present) was performed by similar recording beams and a homogeneous sensitizing (UV) beam. All recording experiments were performed using symmetric transmission geometry with the angle between the two recording beams outside the crystal being 42°.

Figure 2 shows typical recording and read–out curves for four different recording strategies in $LiNbO_3$:Fe:Mn. Normal holographic recording was used for the experiment corresponding to Figures 2 (a) and (b), while two–center recording was used for the other two cases (Figures 2 (c) and (d)). We used the highly reduced crystal (XTAL2) for the experiment corresponding to Figure 2 (a), and the oxidized crystal (XTAL1) for the other three cases. The details of the experiments are summarized in the captions of Figure 2.

The computed values for the best obtainable $M'/\#$, S, and $R/\#$ for the four cases shown in Figure 2 are summarized in Table 1. In these computations, we assumed that the reference storage system is composed of $M = 1000$ holograms multiplexed in the same volume of 1 cm × 1 cm × 1 cm with the minimum acceptable diffraction efficiency of each reconstructed plane–wave hologram being $\eta_{min} = 5 \times 10^{-6}$. We also assume that in such a system, we need to have $N_{ph} = 1000$ photons for each 10 μm × 10 μm pixel ($\mathcal{A}_{pixel} = 10^{-6}$ cm^2) at the detector to obtain an acceptable signal to noise ratio. To compute the values shown in Table 1, we performed several experiments for each case, and averaged the values obtained from the individual experiments. In computing $M/\#$ and S, we assumed extraordinary polarization for the recording and read–out light. This causes both $M/\#$ and S to increase by a factor of about $r_{33}/r_{13} \simeq 3$ due to the larger electro–optic coefficient of $LiNbO_3$ for extraordinary polarization. Here, r_{33} and r_{13} are the corresponding electro–optic coefficients of $LiNbO_3$ for extraordinary and ordinary polarizations of the recording (and read–out) beam, respectively. The last row in Table 1 comments about the strength of holographic scattering and fanning as the sources for deterioration of the holograms especially during read–out. Table
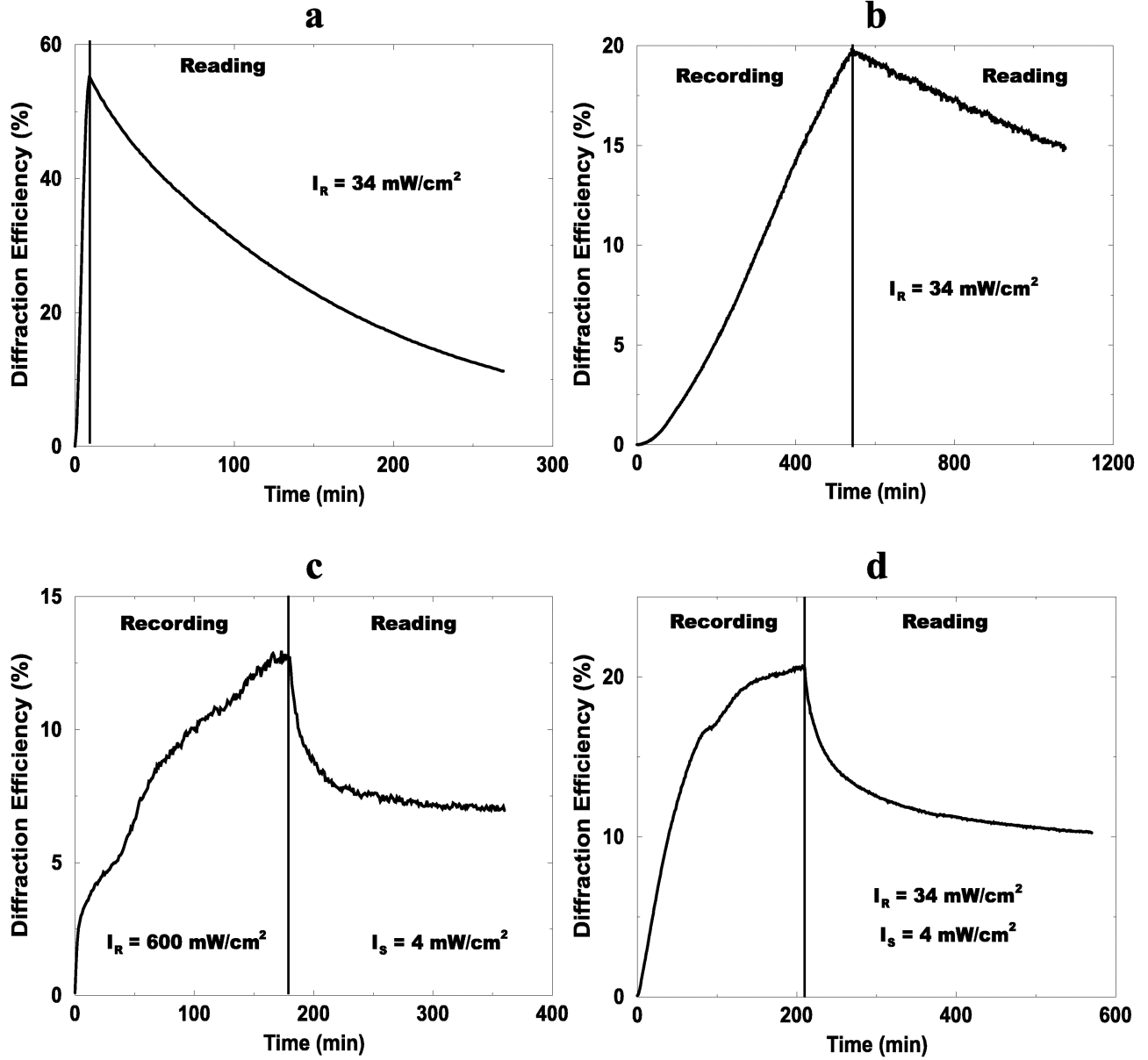
Fig. 2. Recording and read–out curves for a plane–wave hologram in a $LiNbO_3$:Fe:Mn crystal: (a) recording with two plane waves (wavelength 488 nm, intensity of each beam 17 mW/cm^2, ordinary polarization) in the highly reduced sample XTAL2, (b) recording with two plane waves (wavelength 514 nm, intensity of each beam 17 mW/cm^2, ordinary polarization) in the lightly oxidized sample XTAL1, (c) recording with two plane waves (wavelength 633 nm, intensity of each beam 300 mW/cm^2, ordinary polarization) and one sensitizing beam in XTAL1, and (d) recording with two plane waves (wavelength 514 nm, intensity of each beam 17 mW/cm^2, ordinary polarization) and one sensitizing beam in XTAL1. Total recording and sensitizing intensities (I_R and I_S, respectively) are shown in the figures. The intensity of the reading beam during read–out in each case is half of the corresponding recording intensity. The homogeneous sensitizing beam in both (c) and (d) was from a 100 W UV lamp (wavelength 404 nm, intensity 4 mW/cm^2). Erasure of a hologram in all cases was performed by one of the recording beams rotated to result in Bragg–mismatch erasure.

Table 1. Comparison of the performance measures of different recording schemes in a LiNbO$_3$:Fe:Mn crystal. The persistence measure ($R/\#$) is calculated using Eq. 4 with the parameters of the reference system being $M = 1000$, $N_{\text{ph}} = 1000$, $\mathcal{A}_{\text{pixel}} = 10^{-6}$ cm^2 (10 μm $\times$ 10 μm pixels), and $\eta_{\text{min}} = 5 \times 10^{-6}$.

Recording scheme	Normal	Normal	Two–Center	Two–Center
Crystal	XTAL2	XTAL1	XTAL1	XTAL1
Annealing	reduced	oxidized	oxidized	oxidized
Sensitizing wavelength (nm)	–	–	404	404
Sensitizing intensity (mW/cm^2)	–	–	3.8	3.8
Recording wavelength (nm)	488	514	633	514
Recording intensity (mW/cm^2)	31	34	600	34
$(M/\#)/L$ (cm^{-1})	100	55	8	11
S (cm/J)	0.8	0.018	0.01	0.2
$R/\#$ (10^6)	1.5	12	90	0.5
Fanning	severe	small	very small	small
Absorption of recording beams	high	low	low	low

1 reveals the large range of performance that is obtained by using a LiNbO$_3$:Fe:Mn crystal (note that XTAL1 and XTAL2 can be considered as one crystal since they only differ in the oxidation / reduction state). Such a large range of performance cannot be obtained by using a singly–doped LiNbO$_3$ crystal.

5   Discussion

From the numbers for $M/\#$, S, and $R/\#$ in Table 1, it seems that normal recording in the highly reduced crystal, XTAL2 (Figure 2 (a) or second column in Table 1) has the best overall performance. However, fanning and absorption of recording and reading light are severe in this case. Strong fanning in the reduced sample XTAL2 results in the fast deterioration of the stored information. Strong absorption causes high reduction of $M/\#$, S and $R/\#$ when a thick crystal (for example, 1 cm thick) is used. Oxidizing the crystal as well as using a longer recording wavelength (514 nm or 633 nm instead of 488 nm) reduce both fanning and absorption and increase $R/\#$. However, they both reduce the sensitivity considerably as shown in the third column of Table 1 (or Figure 2 (b)). Both fanning and absorption are further reduced by using two–center recording in the oxidized crystal. During recording, the presence of homogeneous sensitizing (UV) light prevents the build up of scattering holograms. During read–out, the insensitivity of the deeper (Mn) traps to the read–out light is the reason for weak fanning. Using two–center recording with UV and red also improves $R/\#$ further. However, sensitivity is very low in two–center recording with UV and red as shown in the fourth column of Table 1 and Figure 2 (c). The very low sensitivity of the two cases shown in Figures 2 (b) and (c) is a major practical disadvantage. From the four cases shown in Figure 2 and Table 1, the last one, i.e., two–center recording with UV and green in the oxidized crystal (Figure 2 (d) or the fifth column in Table 1) has the best overall performance. While both fanning and absorption of recording light are weak in this case, two–center recording with UV and green offers good $M/\#$ and S along with acceptable $R/\#$ for most practical purposes. The combination of good

performance measures in this case is due to the large range of obtainable performance offered by using doubly–doped crystals in holographic recording.

As seen from Table 1, we can obtain huge $R/\#$ (about 100 millions) if we sacrifice sensitivity considerably. On the other hand, we may not need such huge values of $R/\#$ in practical application. Even if we can completely avoid erasure of the holograms during read–out, dark erasure mechanisms cause the decay of the stored information. Therefore, the recorded holograms need to be refreshed from time to time (for example every few months). As a result, $R/\#$ needs to be large enough to ensure that the diffraction efficiency of each holograms does not fall below the minimum acceptable value before the refreshing time. A reasonable value of $R/\#$ with such requirement would be 0.5 millions.

The major challenge in designing a holographic storage system is to appropriately use the trade–offs among $M/\#$, S, and $R/\#$ along with the qualitative measures for absorption and fanning for the desired application. Depending on the application, the main concern might be a subset of these measures. For example, if we do not want to write new information frequently but we need to read the information a lot, we need to use a recording scheme with large $R/\#$ and we can even sacrifice S to obtain better $R/\#$. In such a case, we might use two–center holographic recording with red and UV in a properly oxidized LiNbO$_3$:Fe:Mn crystal (Figure 2 (c)). If we need larger $M/\#$ than that obtained in two–center recording with red and UV, we can sacrifice some persistence ($R/\#$) for $M/\#$ by using two–center holographic recording with green and UV (Figure 2 (d)).

6   Conclusion

In conclusion, we showed that the performance range that can be obtained by using a doubly–doped LiNbO$_3$ crystal is much broader than that obtained in a singly–doped crystal even if recording is performed by only two recording beams without sensitizing light (normal recording). We also showed that by adding a sensitizing beam to the holographic recording system (two–center recording), we can add one dimension for independent performance characteristics (persistence) that further broadens the range of performance characteristics that can be obtained. In two-center recording, three performance parameters ($M/\#$, S, and $R/\#$) can be varied while in normal (single wavelength) recording $R/\#$ is completely dependent on $M/\#$ and S. The main challenge in holographic recording is the appropriate use of the trade–offs among $M/\#$, S, $R/\#$ and qualitative measures like fanning and absorption. Our results show that two–center holographic recording with UV (wavelength 404 nm) and green (wavelength 514 nm) has the best overall performance for practical holographic memory systems. Using this recording scheme in an appropriately annealed 1 cm × 1 cm × 1 cm crystal, we could expect to have $M/\# \simeq 10$, $S \simeq 0.2$ cm/J, $R/\# \simeq 0.4$ millions, as well as weak fanning and light absorption during read–out.

References

1. F. H. Mok, "Angle–Multiplexed Storage of 5000 Holograms in Lithium Niobate," Opt. Lett. **18**, 915–917 (1993).
2. I. McMichael, W. Christian, D. Pletcher, T. Y. Chang, and J. H. Hong, "Compact Holographic Storage Demonstrator with Rapid Access," Appl. Opt. **35**, 2375–2379 (1996).
3. J. Ashley, M.-P. Bernal, M. Blaum, G. W. Burr, H. Coufal, R. K. Grygier, H. Günter, J. A. Hoffnagle, C. M. Jefferson, R. M. MacFarlane, B. Marcus, R. M. Shelby, G. T. Sincerbox, and G. Wittmann, "Holographic Storage Promises High Data Density," Laser Focus World, **32**, pp. 81–93 (November 1996).
4. K. Buse, A. Adibi, and D. Psaltis, "Non–Volatile Holographic Storage in Doubly Doped Lithium Niobate Crystals," Nature **393**, 665–668 (1998).
5. A. Adibi, K. Buse, and D. Psaltis, "Two–center holographic recording," to appear in J. Opt. Soc. Am. B (2001).

6. A. Adibi, K. Buse, and D. Psaltis, "Multiplexing holograms in $LiNbO_3$:Fe:Mn crystals," Opt. Lett. **24**, 652–654 (1999).

7. A. Adibi, K. Buse, and D. Psaltis, "Sensitivity improvement in two–center holographic recording," Opt. Lett. **25**, 539–541 (2000).

8. Y. W. Liu, L. R. Liu, and C. H. Zhou, "Prescription for optimizing holograms in LiNbO3:Fe:Mn," Opt. Lett. **25**, 551–553 (2000).

9. X. F. Yue, A. Adibi, T. Hudson, K. Buse, and D. Psaltis, "Role of cerium in lithium niobate for holographic recording," J. Appl. Phys. **87**, 4051–4055 (2000).

10. Y. W. Liu, L. R. Liu, C. H. Zhou, and L. Y. Xu, "Nonvolatile photorefractive holograms in LiNbO3:Cu:Ce crystals," Opt. Lett. **25**, 908–910 (2000).

11. Y. W. Liu, L. R. Liu, C. H. Zhou, and L. Y. Xu, "Experimental study of non-volatile holographic storage in doubly- and triply-doped lithium niobate crystals," Opt. Commun. **181**, 47–52 (2000).

12. F. H. Mok, G. W. Burr, and D. Psaltis, "System Metric for Holographic Memory Systems," Opt. Lett. **21**, 896–898 (1996).

13. P. Günter and J.-P. H. (eds.), *Topics in Applied Physics: Photorefractive Materials and their Applications I*, **61**. Springer Verlag, 1987.

14. A. Adibi, K. Buse, and D. Psaltis, "System measure for persistence in holographic recording and application to singly–doped and doubly–doped lithium niobate," to appear in Appl. Opt. (2001).

15. D. Psaltis, D. Brady, and K. Wagner, "Adaptive Optical Networks using Photorefractive Crystals," Appl. Opt. **27**, 1752–1759 (1988).

16. E. Chuang, W. Liu., J. J. P. Drolet, and D. Psaltis, "Holographic random access memory (HRAM)," Proceedings of the IEEE **87**, 1931–1940 (1999).

17. A. Adibi, K. Buse, and D. Psaltis, "Effect of annealing in two–center holographic recording," Appl. Phys. Lett. **74**, 3767–3769 (1999).